BJPS

Brazilian Journal of
Pharmaceutical Sciences

http://dx.doi.org/10.1590/s2175-97902025e24279

Article

Orlistat, an anti-obesity drug, suppressed osteosarcoma progression and potentiated pd1ab immune checkpoint blockade therapy via upregulation of serpinf1

Chan Wang[1], Binbo Fang[2], Hanzhang Fu[2], Shumin Li[1]*

[1]Department of orthopedics, Yuhuan Second People's Hospital, Yuhuan, Zhejiang, China,
[2]Department of Medicine, Taizhou University, Zhejiang, China

Orlistat(Orli) is a safe and effective drug for obesity treatment approved by the Food and Drug Administration (FDA) in the US. Recently, Orli has been reported to exert considerable antitumor effects in amount types of malignancy. However, its role in osteosarcoma (OS) progression and its clinical significance in tumor therapy such as immune therapy remains largely unknown. In this study, we detected the effect of Orli exerted on OS progression using CCK-8 assay, wound-healing assay, Enzyme-linked immunosorbent assay (ELISA), cell transfection and xenograft growth assay. The result indicated that by upregulating Serpin Family F member 1 (SERPINF1), a multifunctional protein, OS inhibited OS progression via suppressing proliferation, colony-forming, migration and angiogenesis ability of OS cells *in vitro* and *in vivo*. More importantly, Orli potentiated programmed death1 antibody (PD1ab) immune checkpoint blockade therapy and may candidate as a potential drug in OS therapy.

Keywords: Orlistat. Osteosarcoma. SERPINF1. Programmed death1 antibody.

INTRODUCTION

Osteosarcoma (OS) is the most frequent and primary malignant tumor of bone which often occurs children and adolescents (Ritter, Bielack, 2010; Zhong *et al*., 2020). Due to the difficulty in radically zapping the tumor, easiness in producing chemotherapy resistance and metastasizing to the lung, the prognosis of OS is poor (Jafari *et al*., 2020, Smrke *et al*., 2021, Zhao *et al*., 2021). Among childhood malignancies, the 5-year survival rate of patients with OS ranks the second lowest (Siegel, Miller, Jemal, 2020). OS patients successfully received stand surgery (mainstay of curative OS treatment), the 5-year survival rate is less than 20% (Bernthal *et al*., 2012, Link *et al*., 1986). Furthermore, due to the high toxicity and drug-resistance of chemotherapy, even OS patients can receive both standard surgery (mainstay of curative OS treatment) and intensive adjuvant chemotherapy, the 5-year survival rate showed not much improvement which remains less than 25% (Link *et al*., 1986, Meyers *et al*., 2011). As a promising therapeutic strategy, immune checkpoint blockades(ICBs) including monoclonal antibodies programmed death receptor-1 antibody (PD1ab), anti-cytotoxic T lymphocyte antigen-4 antibody (CTLA4ab) that are on the basis of up-regulating the immune responses (Meftahpour *et al*., 2022). Immune checkpoints (ICPs) are molecules of protein that negatively regulate immune activity when bound to their ligand abnormally expressed on tumor cells, which promoted the immune evasion of malignancy (Zhang, Zheng, 2020). Utilizing blockades such as PD1ab and CTLA4ab for improves the anti-tumors activity of T cells and exerts minimal cytotoxicity on healthy tissue (Li, Chan, Chen, 2019). Indeed, owing to its high and long-lasting therapeutic effect, more and more ICBs such as ipilimumab and nivolumab were permitted to treat advanced melanoma, lung cancer and bladder cancer (Hellmann *et al*., 2019, Ott *et al*., 2020, Rohaan *et al*., 2022). However, due to the low response to ICBs, only small proportion of OS patients can obtain satisfied prognostic benefit from

***Correspondence:** S. Li, Department of Orthopedics, Yuhuan Second People's Hospital, No.77, Environmental Protection Middle Road, Chumen Town, Yuhuan City, Taizhou City, Zhejiang, China, E-mail: 15395761515@163.com, https://orcid.org/0009-0005-0118-8601.

this advanced treatment (Chen *et al*., 2021a). There is an urgent requirement to explore effective and safe potential therapies to augment therapeutic efficiency of ICBs for patients with OS.

Orlistat (Orli) is a safe and effective drug for obesity treatment approved by the Food and Drug Administration (FDA) in the US (2006) (Heck *et al*., 2000). Its primary function is to reducing the absorption of fats from the human diet by potently inhibiting fatty acid synthase (FASN) and activating adipose triglyceride lipase (ATGL) (Chandra *et al*., 2020). Interestingly, owe to its effects on lipid metabolism, Orli has been reported to exert considerable antitumor effects in amount types of malignancy *in vitro* and *in vivo*, including colorectal cancer, prostate cancer, lung cancer, ovarian cancer, cervical cancer and hepatocellular carcinoma (Peng *et al*., 2018, Qu *et al*., 2021, Shang *et al*., 2022, Wei *et al*., 2023, Zhou *et al*., 2021). Moreover, several researches have reported that Orli could significantly promotes the therapeutic effect of chemotherapeutic agents such as oxaliplatin and targeted drugs sorafenib (Li *et al*., 2023; Zhang *et al*., 2022). However, the role of Orli in OS pathogenesis and its clinical significance in immune therapy, such as in combination with ICBs for the treatment of OS, remains largely unknown.

We chose to focus on Serpin family F member 1 (SERPINF1), which is a Serine protease inhibitor family protein showing no inhibiting function against serine protease but shown to be involved in lipid metabolism (Ren, Jie, Talbot, 2005). Both Orli and expression of SERPINF1 took part in modulating lipid metabolism, while their possible association were not determined. SERPINF1 is reportedly to have anti-angiogenesis, anti-tumor, and anti-metastasis properties in several types of cancer such as melanoma, breast cancer and cholangiocarcinoma (Abe *et al*., 2008, Carpino *et al*., 2021, Mao *et al*., 2020). Interestingly, SERPINF1 seemed to demonstrated bidirectional function in different cancers. In esophageal squamous cell carcinoma, SERPINF1 possessed an opposite effect on tumor progression (Chen *et al*., 2021b). Moreover, SERPINF1 was reported to induced resistance to PD1ab in colorectal and bladder cancer (Denis *et al*., 2022). Accounting of its role in lipid metabolism and bidirectional properties in various tumors, it is worthy to explore whether and how SERPINF1 is involved in Orli function acting on OS.

In conclusion, the role of Orli in OS pathogenesis and its clinical significance in immune therapy such as in combination with PD1ab for OS has not yet been studied. Therefore, in this study, we aimed to investigate the antitumor activity and related molecular mechanism of Orli and uncover its role in ICBs therapy on OS.

MATERIAL AND METHODS

Cell lines and culture methods

The human OS cell lines, MG63, U20S, Saos-2 and HOS, and the murine OS cell line K7M2 were purchased from Pricella and cultured in DMEM except for Saos-2 in McCoys'5A containing 10% FBS and 1%penicillin–streptomycin combination. The above OS cells lines were cultured at 37℃ in a 5% CO_2 humidified incubator. The human normal osteoblast cell line hFOB1.19 were obtained from Meisen and cultured in DMEM/F12 with 10% FBS at 34℃ in a 5% CO_2 humidified incubator. All cell lines have been undergone mycoplasma test and the results were all negative.

Animal study

All experimentations on animals were abide by the Care and Use of Laboratory Animals of the National Institutes of Health (NIH) guidelines approved by the Animal Experimental Committee of the Taizhou University.

For OS xenograft model, 1-5×10^6 Saos-2 and HOS cells were digested by pancreatin and added into 100 μL PBS for each BALB/c-nude mouse (female, 4-5 weeks, 17-19 g, a total of 12 were used for Orli treatment on OS xenograft model). The subcutaneous cells injection performed in the left back of the mouse. For subcutaneous tumor model in immunocompetent mice, an injection of

0.5-1×10^6 K7M2 cells were conducted in the left back of each wide-type BALB/c mice (female, 5-6 weeks, 18-20g, a total of 12 were used for Orli treatment on K7M2 subcutaneous tumor model, a total of 48 were employed to detect the effect of SERPINF1 knocking down and Orli treatment on K7M2 subcutaneous tumor model). The tumor volume was measured and calculated by the formula: Tumor Volume (mm3) = (length) × $(width)^2$ × 0.5. The weight of mice was also measured and recorded. When the tumor grew to 50-100 mm^3, the mice were randomly divided into different groups according to different treatments: Orli (100mg/kg, intraperitoneally (i.p.), Cat#T0686, TargetMol, Shanghai, China), PD1ab (200μg/per mouse, i.p., Cat#BE0146, Bioxcell, NEOBIOSCIENCE, China). When tumor volume approached roughly 1000 mm^3, or ulceration occurred, mice sacrificed after being anesthetizing by pentobarbital. Subcutaneous tumors were excised and fixed in formalin (10%) for at least 2 days.

Immunohistochemistry (IHC)

After being fixed in formalin (10%) over 48h, the tumors were cut into sections. The sections then undergo deparaffinization and dehydration by utilizing hydrogen peroxide (3%) and sodium citrate buffer. Primary antibody CD8 (1:1000, Cat#ab209775, ABCAM, USA) or CD31 (1:50, Cat#ab28364, ABCAM, USA) was utilized to incubate with the section overnight and the appropriate secondary antibody was subsequently used to block the section for 1h. 3,3'-diaminobenzidine (DAB) staining was conducted after PBS washing three times and then the sections suffered dehydration and stained utilizing with neutral glue. Finally, the sections were photographed, and the number of $CD8^+$ T cells were counted by two researchers. The intratumoral microvessel density (MVD) was counted and calculated by utilizing Optimas image analyzer (Optimas Corporation USA).

Cell viability

K7M2, Saos-2 and MG63 were firstly digested by pancreatin and added into the medium mixed with Orli in different concentration (0,50,100μM) and seeded into 96-well plates with a cell density of 1*10^3 cells per well. After 24h treatment, cell viability was assessed utilizing CCK-8 kits (Cat# CK04, Dojindo Molecular Technologies, Kumamoto, Japan) in different time points (24h,48h,72h,96h,108h). The reaction time of CCK-8 with cells was 2h. Absorbance was measured at 450nm by employing a microplate reader (Bio-Rad Laboratories Inc, USA) and cell viability was calculated using soft Graphpad 9.0.

Colony formation assay

800 cells of Saos-2 and MG63 in 2ml medium mixed with Orli were added into each well of 6-well plates and cultured at 37℃ in a 5% CO2 humidified incubator for 10-14 days. Eventually, the colonies undergo fixation with methyl alcohol and mounted with Giemsa dye. The 6-well plates were photographed, and the number of cell colonies was calculated by Image J.

Wound-healing assay

1-2*10^6 cells of MG63 in 2ml pure medium were firstly added into each well of the 6-well plates and cultured at 37℃ in a 5% CO2 humidified incubator for 1-2 days. When the cells grew into monolayer, two straight wounds were generated using a pipette tip in each well, and the medium was replaced with pure medium mixed with Orli. The wound was photographed at different time points (0,12h,24h,36h). The cell migration was calculated based on the wound area analyzed by software Image J.

Quantitative real-time polymerase chain reaction array assay (Qpcr assay)

After Orli treatment for 48h, the OS cells and human normal osteoblast cell line hFOB1.19 were collected. Total RNAs were extracted using TRIzol

(Cat#15596018CN, Invitrogen, Carlsbad, CA, USA.) and were reversed into cDNA using Prime-Script RT reagent Kit (Cat#2690A, TAKARA, Dalian, China). Quantitative real-time PCR (qPCR) were performed using the SYBR Premix EX TaqTM (Cat#RR42LR, TAKARA, Dalian, China) operated with an ABI 7500 Real-Time PCR system (Applied Bio-systems, Foster City, USA).

Cell transfection

By using Lipofectamine 2000 (Cat#11668-019, Invitrogen, Carlsbad, CA, USA.), the siRNA targeted to SERPINF1 (Si-SERPINF1, the sequence: CCCAAGCT GAAGCTGAGTTAT) which is purchased from Ribobio (Guangzhou, China) for knocking down SERPINF1 expression was transferred into human OS cells according to the manufacturer's instructions. After successful transfection for 48 h, the osteosarcoma cells were collected for the following *in vitro* experiments. The short hairpin RNA (shRNA) induced downregulation of SERPINF1 in murine OS cells was synthesized by Genechem (Shanghai, China) and the sequence is CGAGTCAAATCCAGCTTTGTT. After successfully transferred into package tool cell line HEK293T using Lipofectamine 2000, the recombinant lentiviruses were produced and transfected the targeted OS cells. The OS cells were screened for 7 days with 0.6 mg/mL puromycin. The efficiency of transfection will be examined by qPCR.

Enzyme-linked immunosorbent assay (ELISA)

After Orli treatment for 48h, cellular supernatant of OS cells was collected. The enzyme-linked immunosorbent assay (ELISA) kit (Cat# BMS619-2, Invitrogen, USA) was utilized to detect the VEGF levels according to the manufacturer's instructions. Three independent experiments were performed in the same procedure.

Statistical analysis

Data was collected and was presented as means ± standard deviation. Two-tailed t-test or one-way analysis of variance (ANOVA) were chosen to analysis the difference with two groups or more groups. $p < 0.05$ was considered statistically significant. *$p < 0.05$, **$p < 0.01$, ***$p < 0.001$,****$p < 0.0001$, n.s. not significant.

RESULTS

Orli inhibited the proliferation, colony-forming, migration and angiogenesis ability of OS cells *in vitro*

Amount of reports have demonstrated that Orli is an effective and safe weight-loss agent that affects lipid metabolism, which has long been approved by the FDA in the US. In this study, firstly, CCK-8 assay was conducted to measure the proliferative effects of Orli on OS cells. As is shown in Figure 1A-1C, Orli exerted concentration-dependent anti-proliferative effects on both murine OS cell line K7M2 and human OS cell lines Saos-2 and MG63. The result of colony formation assay suggested that Orli suppressed colony-forming ability of MG63 (Figure 1D). Furthermore, Orli exhibited inhibiting effect on angiogenesis by markedly decreasing the VEGF secretion of MG63 and K7M2 (Figure 1E-1F). According to the wound-healing assay, Orli significantly decreased the migratory potential of MG63 (Figure 1G-1H). In conclusion, the result of this section indicated that Orli suppressed OS progression by inhibiting the proliferation, colony-forming, migration and angiogenesis ability of OS cells *in vitro*.

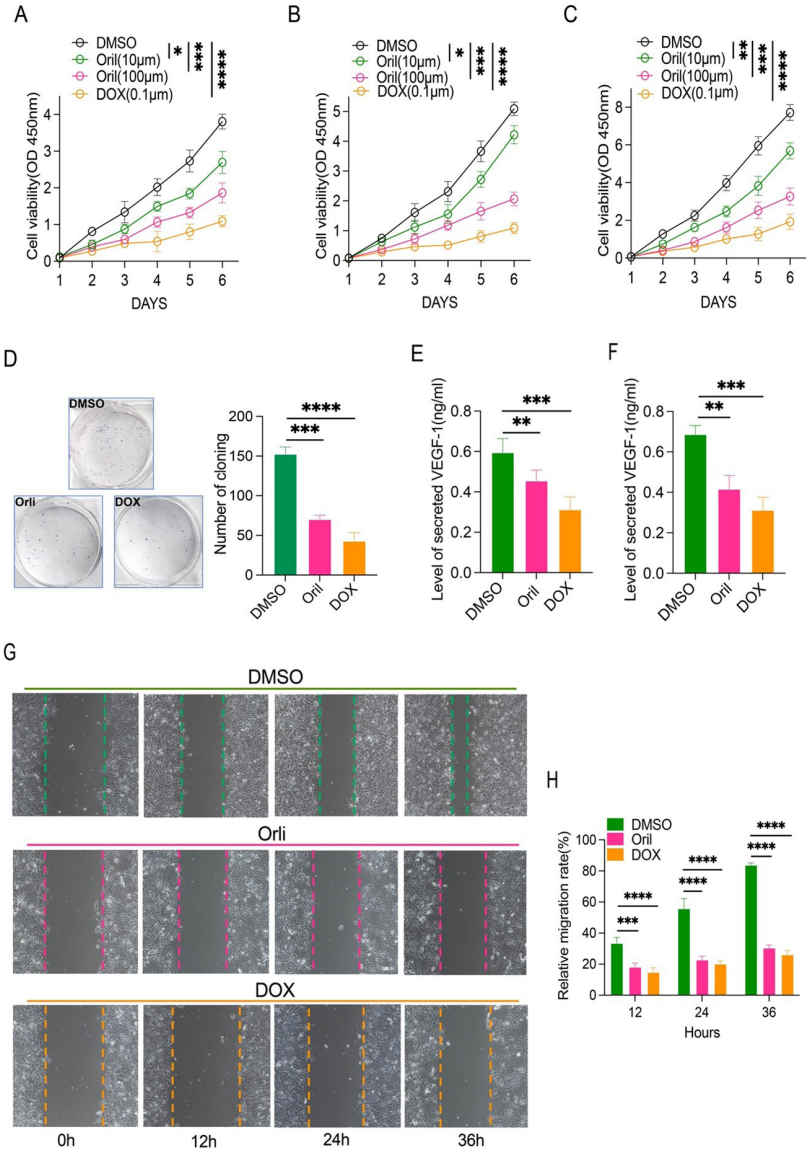

FIGURE 1 - Orli inhibited the proliferation, colony-forming, migration and angiogenesis ability of OS cells *in vitro*. (A-C) Cell viability of K7M2(A), Saos-2 cells (B) and MG63(C) were measured by the CCK-8 assay after with various concentrations of Orli treatment (0 μM, 10 μM, 100 μM) and as DOX (doxorubicin, 0.1μM) as positive control, n=3; (D) Cell colony-formation ability of MG63 cells after treatment with Orli (100 μM) or DOX (doxorubicin, 0.1μM) as positive control, n=3; (E-F) ELISA detection on VEGF secretion of MG63 and K7M2 cells after treatment with Orli (100 μM) or DOX (doxorubicin, 0.1μM); (G-H) Cell migration capacity of MG63 cells after treatment with Orli (100 μM) or DOX (doxorubicin, 0.05μM) as positive control was tested through wound healing assays (G) and their quantitative analysis(H), n=3.

Orli suppressed tumorigenicity of both murine and human OS cells *in vivo*

We next constructed the subcutaneous tumor model to further validate the effect of Orli on the potential of OS tumor formation *in vivo*. In experiments with a syngeneic tumor model utilizing murine OS cells K7M2 (Figure 2A), the tumor volume and weight of the mice received Orli treatment (100mg/kg, i.p. every two days) were significantly reduced compared to the DMSO group (Figure S1A-S1B, Figure 2B-2D). The inhibiting effect of Orli on tumor formation could also

be observed that Orli treatment significantly decreased the density of CD31+ vessels *in vivo* (Figure S1C-S1D). In conclusion, the above result suggested that Orli suppressed OS cell proliferation *in vivo*.

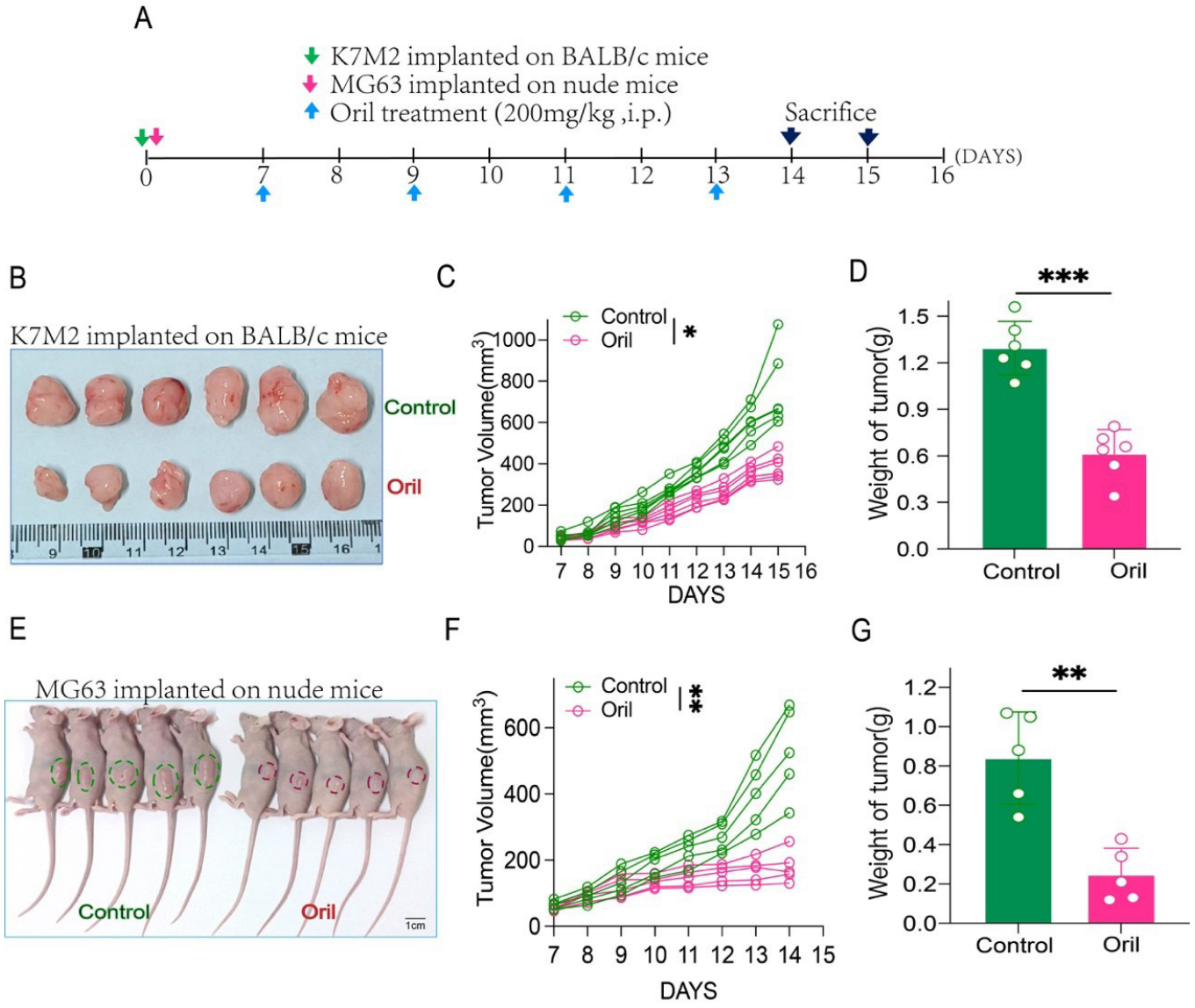

FIGURE 2 - Orli suppressed tumorigenicity of both murine and human OS cells *in vivo*. (A) Schematic representation of Orli treatment on K7M2 tumors on BALB/c mice or MG63 tumors on nude mice; (B) Representative photo of K7M2 subcutaneous tumor models; (C) curve of K7M2 tumor size in each group; (D) weight of K7M2 tumor in each group; (E) Representative photo of MG63 xenograft models; (F) curve of MG63 tumor size in each group; (G) weight of MG63 tumor in each group.

Orli suppressed OS progression via modulating SERPINF1

SERPINF1 was a serine protease with various function including modulating tumor pathogenesis and lipid metabolism which may be a target of Orli. In this section, initially, the result of qPCR detection revealed that SERPINF1 expression level was significantly lower in human OS cells (SAOS-2, U2OS, HOS, and MG63) compared with that in osteoblast cells (hFOB1.19)

(Figure 3A). Moreover, after Orli treatment, the SERPINF1 expression level was significantly upregulated in both MG63 and K7M2 OS cells (Figure 3B-3C). After successfully knocked down SERPINF1 in K7M2 and MG63 (Figure 3D), the result of CCK-8 assay indicated that, SERPINF1 knock down promoted proliferation ability of K7M2 compared with that of untreated cells. When adding with Orli, the inhibiting effect of Orli represented not significant between the Si-SERPINF1 group and Orli+Si-SERPINF1 group (Figure 3E). The similar result could be observed in the human OS cells MG63 (Figure 3F). Furthermore, the result of ELISA detection indicated that, SERPINF1 knock down promoted VEGF secretion of K7M2 compared with that of control cells. However, the VEGF secretion of Orli+Si-SERPINF1 cells did not differ significantly from that of Si-SERPINF1 group cells (Figure 3G). Similar phenomenon was observed in human OS cell line MG63 (Figure 3H). In general, the above outcomes assisted to prove that Orli inhibited the proliferation and angiogenesis ability of OS cells.

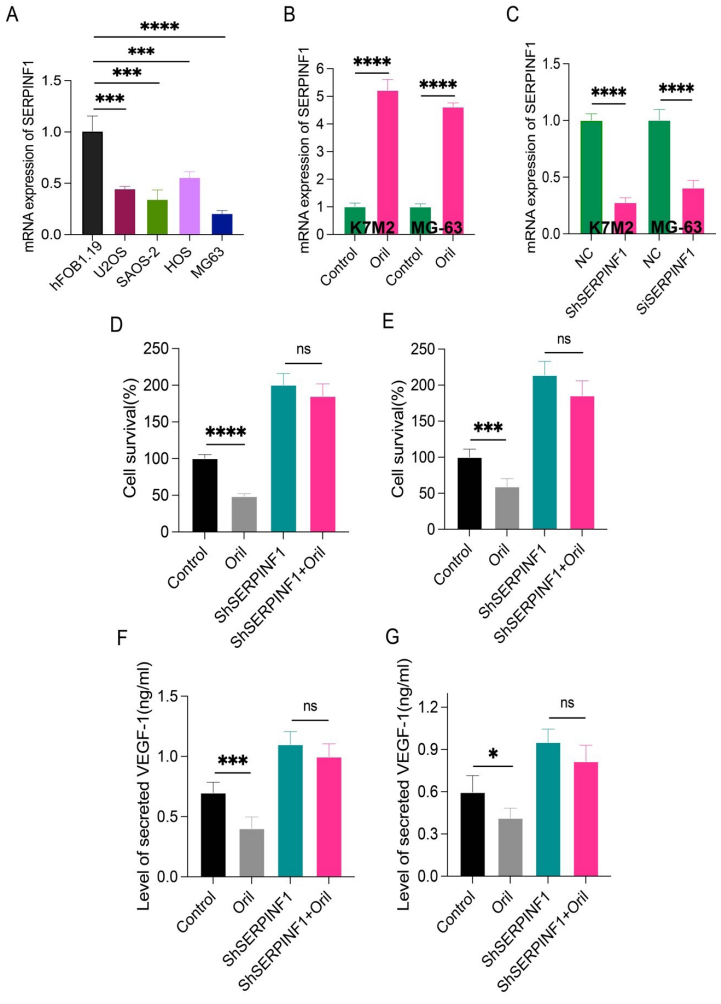

FIGURE 3 - Orli suppressed OS progression via modulating SERPINF1. (A) SERPINF1 expression in OS cell lines (Saos-2, HOS , U2OS, and MG63) and a human normal osteoblast cell line (hFOB1.19) detected by Qpcr; (B) SERPINF1 expression in MG63 (B) after Orli treatment (10μM, 50μM, 100μM) detected by Qpcr; (C) The efficiency of SERPINF1 knock down detected by Qpcr; (D-E) Cell viability of MG63 (D) and K7M2(E) after knocking down SERPINF1 expression and Orli (100 μM); treatment; (F-G)VEGF secretion of MG63 (F) and K7M2(G) after knocking down SERPINF1 expression and Orli (100 μM).

Orli enhanced PD1ab therapy by upregulating SERPINF1 expression.

The aforementioned results suggested that Orli could significantly impaired the proliferation and angiogenesis ability of OS cells via SERPINF1. Considering the strong association between angiogenesis and T cells, and furthermore, the IHC detection revealed that Orli significantly increased the number of infiltrated $CD8^+$ T cells in K7M2 tumors (Figure S1E-S1F), we hypothesized that Orli may exert a synergetic enhancement on PD1ab therapy. In this section, by employing a syngeneic murine OS cancer model (Figure 4A-4B), we found that Orli treatment could significantly inhibit OS growth compared with that of the DMSO group. Furthermore, the combination of Orli and PD1ab demonstrated an enhanced effect on tumor inhibition (Figure 4C, 4E). However, when successfully knocked down SERPINF1, the tumor growth rate of Sh-SERPINF1 group accelerated compared with that of DMSO group. In addition, the tumor size and weight of Sh-SERPINF1 group presented to be comparable with the Orli+Sh-SERPINF1 group or PD1ab+Sh-SERPINF1 Group. More importantly, the tumor size and weight of PD1ab+Sh-SERPINF1 did not differ from that of Orli+PD1ab+Sh-SERPINF1 group (Figure 4D, 4E). In conclusion, Orli may potentiate PD1ab therapy via modulating SERPINF1expression.

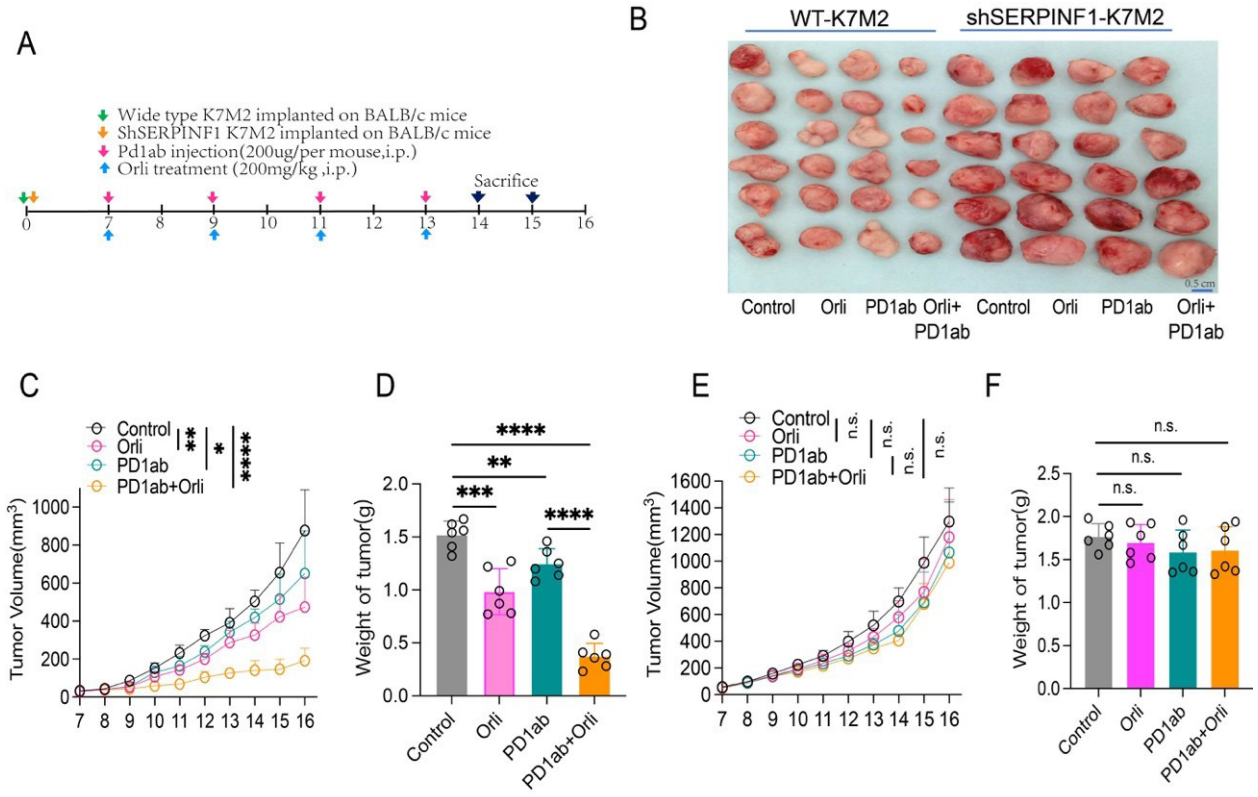

FIGURE 4 - Orli enhanced PD1ab therapy by upregulating SERPINF1 expression. (A) Scheme representing the experimental procedure including Orli (100mg/kg, i.p.) and PD1ab (200μg per mouse, i.p.) treatment on BALB/C mice; (B) Representative images of wild-type K7M2 tumors and SH-SERPINF1 tumors after treatment; (C-D) Curve growth curves of wild-type K7M2 tumors(C) and SH-SERPINF1 tumors (D); (D) tumor burdens of wild-type K7M2 tumors and SH-SERPINF1 tumors after treatment.

DISCUSSION

In this study, Orli, a FDA-approved anti-obesity drug, was demonstrated to inhibit the proliferative, migratory and angiogenesis abilities of OS both *in vitro* and *in vivo* and potentiate ICBs PD1ab therapy via upregulation of SERPINF1. This is the first research to investigate the anti-tumor activity and related mechanism of Orli in OS. In general, these findings demonstrated that Orli might be an effective and safe agent for OS therapy, especially in ICBs combination.

Amount of reports have demonstrated that Orli is an effective and safe weight-loss agent that affects lipid metabolism, which has long been approved by the FDA in the US (Tak, Lee, 2021). Besides potently inhibiting impact on FASN and preventing the intestinal absorption of triacylglycerol, Orli was recently reported to exhibit potent antitumor effects *in vitro* and *in vivo* in many types of malignant tumors, including lung cancer (Yang, Qiao, Zhu, 2023), cervical cancer (Nascimento *et al*., 2022; C. Zhang *et al*., 2020), breast cancer (Bhargava-Shah *et al*., 2016; Menendez, Vellon, Lupu, 2005), gastric cancer (Dowling, Cox, Cenedella, 2009), colorectal cancer (Ye *et al*., 2023) prostate cancer (Wright *et al*., 2017) and hepatocellular carcinoma (Shueng *et al*., 2022). Previous reports of Orli in cancer research mostly were focus on the FASN inhibition (Papaevangelou *et al*., 2018, Schcolnik-Cabrera *et al*., 2018), anti-angiogenic effects (Bruning *et al*., 2018) and potential to promote apoptotic and ferroptosis (Zhou *et al*., 2021). For example, some scholars reported that Orli inhibited the proliferation and viabilities of lung cancer cells and induced ferroptosis-like cell death *in vitro* and *in vivo* (Zhou *et al*., 2021). some researchers found that Orli induce apoptotic and antiangiogenic effects as well as inhibition of fatty acid synthesis in breast cancer cells (Jovankić *et al*., 2023). However, laboratory research of Orli on OS prevention is rare. The function and mechanism of Orli in OS pathogenesis and its clinical significance especially in ICBs therapy, remains unknown. In this research, similar to the result previously reported, we found that Orli directly inhibited proliferative and migratory abilities of human OS cells lines both *in vitro* and *in vivo*. Furthermore, Orli shows additional function in modulating the tumor microenvironment, which was demonstrated to increase $CD8^+$ T cells into the tumors and show synergistic activity with PD1ab therapy in immunocompetent mice. In conclusion, the phenotypic research revealed that Orli could prevent OS progression, induce $CD8^+$ T cells infiltration and enhance PD1ab therapy.

A recent report demonstrated that Orli potentiated PD-1/PD-L1 antibody therapeutic effect in colorectal and bladder cancer model which is similar with our findings while the mechanism is quite different. The researcher proposed that SERPINF1 might be a key a factor involved in free fatty acids (FFA) metabolic pathways and was responsible for the resistance to PD-1/PD-L1 antibody therapy (Denis *et al*., 2022). Interestingly, in our research, we verified that SERPINF1, the potential target of Orli, exerted distinct effect on OS progression and PD1ab inhibition. Although some reports indicated that presence of SERPINF1 suppressed proliferation and migration of cancer cells such as melanoma (Abe *et al*., 2004), other researchers have demonstrated an opposite impact on OS cells Saos-2 (Ek *et al*., 2007), which is consistent with our findings. In this study, SERPINF1 represented low expression in OS compared with human normal osteoblast cell hFOB1.19 and Orli significantly upregulated SERPINF1 expression in two human OS cell lines. Knocking down of SERPINF1 promoted proliferation, migration and reducing infiltration of CD8+ T cells in tumor tissue, while the adding of Orli reverse these phenotypes and enhanced PD1ab inhibition. In addition, knocking down of SERPINF1 demonstrated a stimulatory effect on VEGF secretion of human OS cells, and Orli treatment neutralized this phenomenon instead. In tumor microenvironment, pro-angiogenic cytokines such as VEGF are abnormally upregulated and drive angiogenesis (Qin *et al*., 2020). As a result, the leaky and immature vessels result in high interstitial fluid pressure which prevents blood perfusion and immune cell infiltration (Böckelmann, Schumacher, 2019). In addition, VEGF could induce

the exhaustion of T cells (Lee *et al*., 2020). More and more angiogenesis inhibitor plus PD-1/PD-L1 antibody strategies are tested by clinical trials and waiting approval by the NMPA or FDA (Yi *et al*., 2022). Consistently, our present research assisted to prove that Orli reduced VEGF secretion via modulating SERPINF1, resulting in increased $CD8^+$ T cells infiltration and sensitization in PD1ab inhibition on OS. However, to explore this in more depth, detail experiments in mechanism study are warranted in the future.

Limitation

Our results provided a preliminary and encouraging strategy about Orli combined with PD1ab therapy (Figure 5) but remained some limitation, such as more such as more direct evidence is warranted to verify that Orli modulated tumor microenvironment and prevented OS progression via SERPINF1, in consideration of the time and cost of the trial, we can only explore this meachanism by simple and feasible experiments of the present kind. Further investigation on the mechanism and related clinical trials should be conducted in the future.

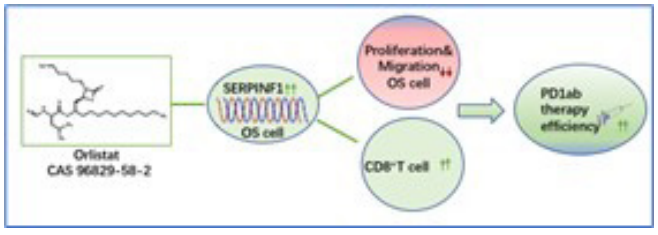

FIGURE 5 - A schematic diagram illustrating Orli impaired the proliferation, migration and angiogenesis capacity of OS cell and potentiate PD1ab therapy via upregulating SERPINF1.

ACKNOWLEDGEMENTS

Not applicable.

FUNDING

The Taizhou Municipal Science and Technology Bureau (No.21ywb112)

ETHICAL APPROVAL AND CONSENT TO PARTICIPATE

All experiments performed in this study are in accordance with the ethical standards of the Declaration of Helsinki. Informed consent is not applicable for all data were going to be analyzed anonymously. All animal experiments were approved by the Animal Care and Use Committee of Taizhou University and complied with the guidelines for the ethical treatment of animals.

COMPETING INTERESTS

The authors declare that they have no competing interests.

AUTHORS' CONTRIBUTIONS

S.L led study design and prepared the manuscript; C.W, B.F and H.F carried out the experiments; B.F and H.F performed statistical analysis; S.L performed data analysis and interpretation; All authors read and approved the final manuscript.

REFERENCES

Abe R, Fujita Y, Yamagishi S, Shimizu H. Pigment epithelium-derived factor prevents melanoma growth via angiogenesis inhibition. Curr Pharm Des. 2008;14(36):3802-9.

Abe R, Shimizu T, Yamagishi S, Shibaki A, Amano S, Inagaki Y, et al. Overexpression of pigment epithelium-derived factor decreases angiogenesis and inhibits the growth of human malignant melanoma cells in vivo. Am J Pathol. 2004;164(4):1225-32.

Bernthal NM, Federman N, Eilber FR, Nelson SD, Eckardt JJ, Eilber FC, et al. Long-term results (>25 years) of a randomized, prospective clinical trial evaluating chemotherapy in patients with high-grade, operable osteosarcoma. Cancer. 2012;118(23):5888-93.

Bhargava-Shah A, Foygel K, Devulapally R, Paulmurugan R. Orlistat and antisense-miRNA-loaded PLGA-PEG nanoparticles for enhanced triple negative breast cancer therapy. Nanomedicine (Lond). 2016;11(3):235-47.

Böckelmann LC, Schumacher U. Targeting tumor interstitial fluid pressure: will it yield novel successful therapies for solid tumors? Expert Opin Ther Targets. 2019;23(12):1005-14.

Bruning U, Morales-Rodriguez F, Kalucka J, Goveia J, Taverna F, Queiroz KCS, et al. Impairment of Angiogenesis by Fatty Acid Synthase Inhibition Involves mTOR Malonylation. Cell Metab. 2018;28(6):866-80. e15.

Carpino G, Cardinale V, Di Giamberardino A, Overi D, Donsante S, Colasanti T, et al. Thrombospondin 1 and 2 along with PEDF inhibit angiogenesis and promote lymphangiogenesis in intrahepatic cholangiocarcinoma. J Hepatol. 2021;75(6):1377-86.

Chandra P, Enespa, Singh R, Arora PK. Microbial lipases and their industrial applications: a comprehensive review. Microb Cell Fact. 2020;19(1):169.

Chen C, Xie L, Ren T, Huang Y, Xu J, Guo W. Immunotherapy for osteosarcoma: Fundamental mechanism, rationale, and recent breakthroughs. Cancer Lett. 2021a;500:1-10.

Chen Z, Che D, Gu X, Lin J, Deng J, Jiang P, et al. Upregulation of PEDF Predicts a Poor Prognosis and Promotes Esophageal Squamous Cell Carcinoma Progression by Modulating the MAPK/ERK Signaling Pathway. Front Oncol. 2021b;11:625612.

Denis M, Grasselly C, Choffour PA, Wierinckx A, Mathé D, Chettab K, et al. In Vivo Syngeneic Tumor Models with Acquired Resistance to Anti-PD-1/PD-L1 Therapies. Cancer Immunol Res. 2022;10(8):1013-27.

Dowling S, Cox J, Cenedella RJ. Inhibition of fatty acid synthase by Orlistat accelerates gastric tumor cell apoptosis in culture and increases survival rates in gastric tumor bearing mice in vivo. Lipids. 2009;44(6):489-98.

Ek ET, Dass CR, Contreras KG, Choong PF. Pigment epithelium-derived factor overexpression inhibits orthotopic osteosarcoma growth, angiogenesis and metastasis. Cancer Gene Ther. 2007;14(7):616-26.

Heck AM, Yanovski JA, Calis KA. Orlistat, a new lipase inhibitor for the management of obesity. Pharmacotherapy. 2000;20(3):270-9.

Hellmann MD, Paz-Ares L, Bernabe Caro R, Zurawski B, Kim SW, Carcereny Costa E, et al. Nivolumab plus Ipilimumab in Advanced Non-Small-Cell Lung Cancer. N Engl J Med. 2019;381(21):2020-31.

Jafari F, Javdansirat S, Sanaie S, Naseri A, Shamekh A, Rostamzadeh D, et al. Osteosarcoma: A comprehensive review of management and treatment strategies. Ann Diagn Pathol. 2020;49:151654.

Jovankić JV, Nikodijević DD, Milutinović MG, Nikezić AG, Kojić VV, Cvetković AM, et al. Potential of Orlistat to induce apoptotic and antiangiogenic effects as well as inhibition of fatty acid synthesis in breast cancer cells. Eur J Pharmacol. 2023;939:175456.

Lee WS, Yang H, Chon HJ, Kim C. Combination of anti-angiogenic therapy and immune checkpoint blockade normalizes vascular-immune crosstalk to potentiate cancer immunity. Exp Mol Med. 2020;52(9):1475-85.

Li B, Chan HL, Chen P. Immune Checkpoint Inhibitors: Basics and Challenges. Curr Med Chem. 2019;26(17):3009-25.

Li Y, Yang W, Zheng Y, Dai W, Ji J, Wu L, et al. Targeting fatty acid synthase modulates sensitivity of hepatocellular carcinoma to sorafenib via ferroptosis. J Exp Clin Cancer Res. 2023;42(1):6.

Link MP, Goorin AM, Miser AW, Green AA, Pratt CB, Belasco JB, et al. The effect of adjuvant chemotherapy on relapse-free survival in patients with osteosarcoma of the extremity. N Engl J Med. 1986;314(25):1600-6.

Mao Y, Zhu L, Huang Z, Luo C, Zhou T, Li L, et al.

Stem-like tumor cells involved in heterogeneous vasculogenesis in breast cancer. Endocr Relat Cancer. 2020;27(1):23-39.

Meftahpour V, Aghebati-Maleki A, Fotouhi A, Safarzadeh E, Aghebati-Maleki L. Prognostic significance and therapeutic potentials of immune checkpoints in osteosarcoma. Excli j. 2022;21:250-68.

Menendez JA, Vellon L, Lupu R. Antitumoral actions of the anti-obesity drug orlistat (XenicalTM) in breast cancer cells: blockade of cell cycle progression, promotion of apoptotic cell death and PEA3-mediated transcriptional repression of Her2/neu (erbB-2) oncogene. Ann Oncol. 2005;16(8):1253-67.

Meyers PA, Healey JH, Chou AJ, Wexler LH, Merola PR, Morris CD, et al. Addition of pamidronate to chemotherapy for the treatment of osteosarcoma. Cancer. 2011;117(8):1736-44.

Nascimento J, Mariot C, Vianna DRB, Kliemann LM, Chaves PS, Loda M, et al. Fatty acid synthase as a potential new therapeutic target for cervical cancer. An Acad Bras Cienc. 2022;94(2):e20210670.

Ott PA, Hu-Lieskovan S, Chmielowski B, Govindan R, Naing A, Bhardwaj N, et al. A Phase Ib Trial of Personalized Neoantigen Therapy Plus Anti-PD-1 in Patients with Advanced Melanoma, Non-small Cell Lung Cancer, or Bladder Cancer. Cell. 2020;183(2):347-62.e24.

Papaevangelou E, Almeida GS, Box C, deSouza NM, Chung YL. The effect of FASN inhibition on the growth and metabolism of a cisplatin-resistant ovarian carcinoma model. Int J Cancer. 2018;143(4):992-1002.

Peng H, Wang Q, Qi X, Wang X, Zhao X. Orlistat induces apoptosis and protective autophagy in ovarian cancer cells: involvement of Akt-mTOR-mediated signaling pathway. Arch Gynecol Obstet. 2018;298(3):597-605.

Qin S, Yi M, Jiao D, Li A, Wu K. Distinct Roles of VEGFA and ANGPT2 in Lung Adenocarcinoma and Squamous Cell Carcinoma. J Cancer. 2020;11(1):153-67.

Qu Z, Ren Y, Shen H, Wang H, Shi L, Tong D. Combination Therapy of Metastatic Castration-Recurrent Prostate Cancer: Hyaluronic Acid Decorated, Cabazitaxel-Prodrug and Orlistat Co-Loaded Nano-System. Drug Des Devel Ther. 2021;15:3605-16.

Ren JG, Jie C, Talbot C. How PEDF prevents angiogenesis: a hypothesized pathway. Med Hypotheses. 2005;64(1):74-8.

Ritter J, Bielack SS. Osteosarcoma. Ann Oncol. 2010;21 Suppl 7:vii320-5.

Rohaan MW, Borch TH, van den Berg JH, Met Ö, Kessels R, Geukes Foppen MH, et al. Tumor-Infiltrating Lymphocyte Therapy or Ipilimumab in Advanced Melanoma. N Engl J Med. 2022;387(23):2113-25.

Schcolnik-Cabrera A, Chávez-Blanco A, Domínguez-Gómez G, Taja-Chayeb L, Morales-Barcenas R, Trejo-Becerril C, et al. Orlistat as a FASN inhibitor and multitargeted agent for cancer therapy. Expert Opin Investig Drugs. 2018;27(5):475-89.

Shang C, Li Y, He T, Liao Y, Du Q, Wang P, et al. The prognostic miR-532-5p-correlated ceRNA-mediated lipid droplet accumulation drives nodal metastasis of cervical cancer. J Adv Res. 2022;37:169-84.

Shueng PW, Chan HW, Lin WC, Kuo DY, Chuang HY. Orlistat Resensitizes Sorafenib-Resistance in Hepatocellular Carcinoma Cells through Modulating Metabolism. Int J Mol Sci. 2022;23(12).

Siegel RL, Miller KD, Jemal A. Cancer statistics, 2020. CA Cancer J Clin. 2020;70(1):7-30.

Smrke A, Anderson PM, Gulia A, Gennatas S, Huang PH, Jones RL. Future Directions in the Treatment of Osteosarcoma. Cells. 2021;10(1).

Tak YJ, Lee SY. Anti-Obesity Drugs: Long-Term Efficacy and Safety: An Updated Review. World J Mens Health. 2021;39(2):208-21.

Wei W, Qin B, Wen W, Zhang B, Luo H, Wang Y, et al. FBXW7β loss-of-function enhances FASN-mediated lipogenesis and promotes colorectal cancer growth. Signal Transduct Target Ther. 2023;8(1):187.

Wright C, Iyer AKV, Kaushik V, Azad N. Anti-Tumorigenic Potential of a Novel Orlistat-AICAR Combination in Prostate Cancer Cells. J Cell Biochem. 2017;118(11):3834-45.

Yang T, Qiao S, Zhu X. High-dose radiation-resistant lung cancer cells stored many functional lipid drops through JAK2/p-STAT3/FASN pathway. J Cancer Res Clin Oncol. 2023;149(15):14169-83.

Ye M, Hu C, Chen T, Yu P, Chen J, Lu F, et al. FABP5 suppresses colorectal cancer progression via mTOR-mediated autophagy by decreasing FASN expression. Int J Biol Sci. 2023;19(10):3115-27.

Yi M, Zheng X, Niu M, Zhu S, Ge H, Wu K. Combination strategies with PD-1/PD-L1 blockade: current advances and future directions. Mol Cancer. 2022;21(1):28.

Zhang C, Liao Y, Liu P, Du Q, Liang Y, Ooi S, et al. FABP5 promotes lymph node metastasis in cervical cancer by reprogramming fatty acid metabolism. Theranostics. 2020;10(15):6561-80.

Zhang Q, Zhou Y, Feng X, Gao Y, Huang C, Yao X. Low-dose orlistat promotes the therapeutic effect of oxaliplatin in colorectal cancer. Biomed Pharmacother. 2022;153:113426.

Zhang Y, Zheng J. Functions of Immune Checkpoint Molecules Beyond Immune Evasion. Adv Exp Med Biol. 2020;1248:201-26.

Zhao X, Wu Q, Gong X, Liu J, Ma Y. Osteosarcoma: a review of current and future therapeutic approaches. Biomed Eng Online. 2021;20(1):24.

Zhong J, Si L, Geng J, Xing Y, Hu Y, Jiao Q, et al. Chondromyxoid fibroma-like osteosarcoma: a case series and literature review. BMC Musculoskelet Disord. 2020;21(1):53.

Zhou W, Zhang J, Yan M, Wu J, Lian S, Sun K, et al. Orlistat induces ferroptosis-like cell death of lung cancer cells. Front Med. 2021;15(6):922-32.

Received for publication on April 12th, 2024
Accepted for publication on September 24th, 2024
Associated Editor: Moacyr Rêgo

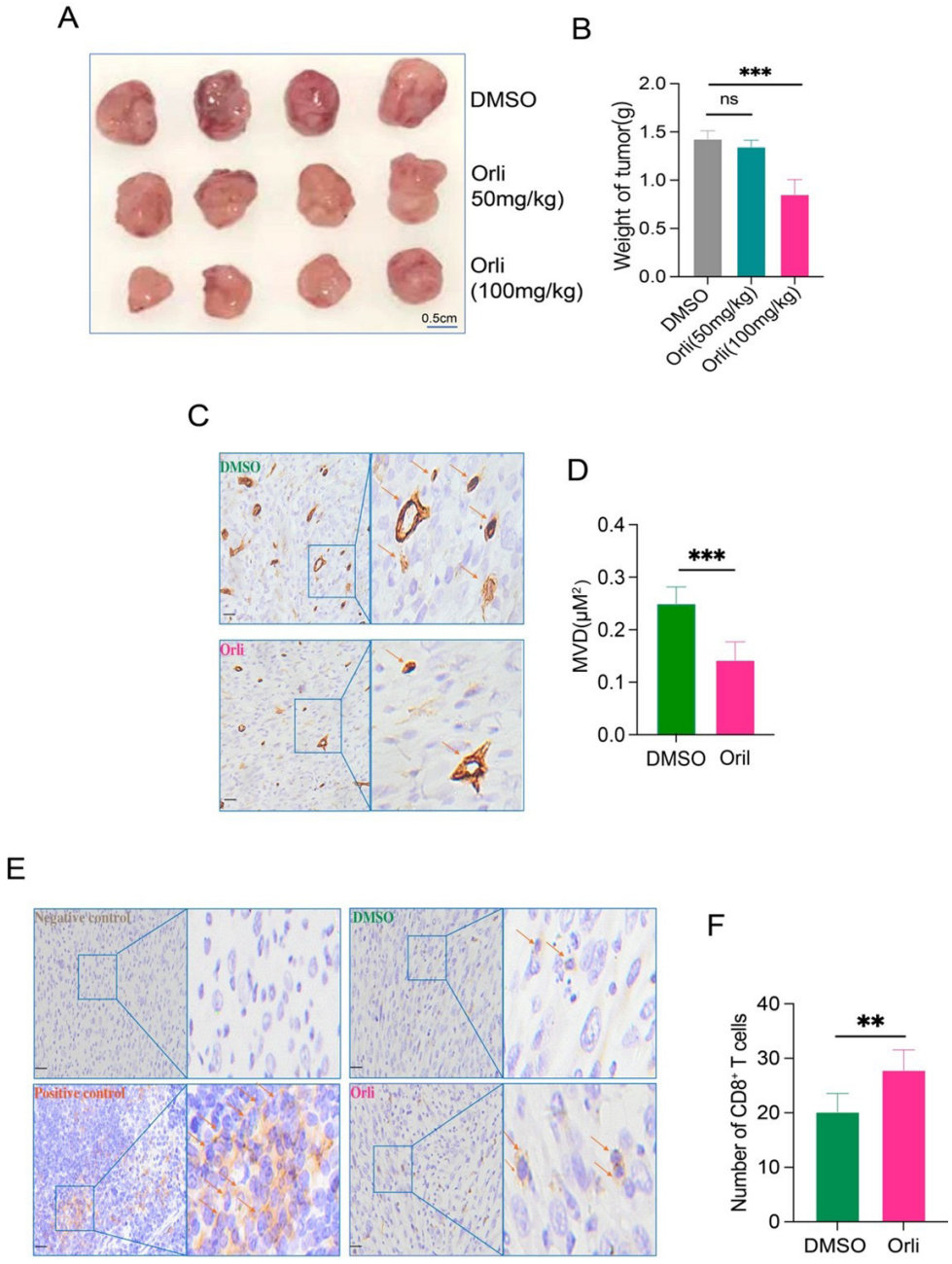

FIGURE S1 - (A) Representative images of K7M2 tumors after treatment with Oril (0, 50mg/kg, 100mg/kg); (B) Weight of tumors; (C–D) IHC analysis of CD31+ vessels of MG63 tumor tissue after Oril (100mg/kg) treatment; (C) Representative IHC images; (D) MVD of tumor tissue; (E–F)IHC analysis of CD8+ T cell infiltration of K7-M2 tumor tissue after Oril treatment; (E) Representative IHC images, negative control, sections without using primary CD8 antibody; positive control: mice spleen section staining with primary CD8 antibody; (F) Number of $CD8^+$ T cell infiltration of K7-M2 tumor tissue after Oril treatment. Scale bar, 20μm. $^{**}p < 0.01$.